Adaptive Voltage-Sensor-Based MPPT for PV System Using SEPIC Converter

[1]Suraj ArunGaikwad, [2]A.P.Kinge
[1]PG Student, [2]Professor
[1,2] BhivarabaiSawant College of Engineering and Research,
Pune, India

Abstract: *In* this paper variable scaling factor for a single ended primary inductance converter is used in adaptive voltage sensor based maximum power point tracking algorithm. The voltage level of PV panel is detected by voltage divider circuit. The most important for every system is to become stable. The method employed in this work can enhance the transient and steady state factor. The solar radiations are not constant; it varies throughout the day so tracking of radiation is difficult for maximum power. This method can track more efficiently and in steady state condition it makes the oscillation low. For testing the result MATLAB/SIMULINK is used in this work.

Index Terms **–Maximum power point tracking (MPPT), Photovoltaic (PV), Single-endedprimary-inductance converter (SEPIC), Voltage Sensor.**

I. INTRODUCTION

Renewable energy source is most powerful source of energy for electric power generation without affecting the environment as it is clean energy. The basic principle of Photovoltaic system is to convert solar energy into electrical energy directly. Due to increased use of PV system in electrical power generation technologies, the problem with PV module is that it shows non-linear I-V & P-V characteristics. Dependency on solar irradiance and atmospheric temperature for power generation is easily shown on I-V & P-V characteristics. The most important is efficiency of PV system which depends on the operating point in the characteristics curve of the PV module. The maximum power operating point (MPOP) of Photovoltaic power generation system changes with solar radiation and temperature, so it is important to design efficient PV system to track the MPOP accurately. Many MPPT techniques have been used in past to increase the efficiency of the PV system [2-20].

The MPPT algorithms and different control techniques have been implemented to extract the maximum power from PV module.

The traditional MPPT methods are used with a fixed perturbation step size determined by the trade-off between efficiency and tracking speed requirements. To minimize the tracking time and to improve steady state performance variable step size MPPT methods are used. The step size is defined as a function of either the derivative of power to voltage eqn or the derivative of power to duty cycle. Adaptive MPPT algorithms improves the efficiency of the system by minimizing the tracking period and power loss in steady state[8],[10].

The most commonly used techniques are P&O and IncCond. In these two methods voltage and current sensors are required. Current sensing is implemented with shunt resistor in differential amplifier configuration.
This paper is organized as follows:

I. Voltage based sensor MPPT with fixed step size and adaptive step size.
II. Analysis for a change in irradiation.
III. Simulation result
IV. Conclusion

II. VOLTAGE SENSOR BASED MPPT FOR SEPTC

For maximum power extraction MPPT controller is important. Due to impedance mismatch it is not possible to operate at peak power point if load is already connected to the PV array. By changing the duty cycle generated from MPPT controller, the converter used to operate at MPP. The bock diagram of a PV system with MPPT controller is shown in Fig.1.
From the P-D characteristics shown in fig.2 it has been observed that at MPP the slope of eqn, eqn to the left side of MPP and eqn to the right side of MPP. For SEPIC converter we used to develop voltage sensor based MPPT algorithm with P-D characteristics using PV module. The motive is to implement this algorithm for SEPIC converter has been derived for both resistive and battery load.

A. Case 1 for Resistive load

Efficiency of the converter can be calculated as

$$\eta = \frac{V_O I_O}{V_{PV} I_{PV}}$$

$$= \frac{V_O I_O}{\frac{V_{PV}}{R_{eq}}} = \left(\frac{V_O}{V_{PV}}\right)^2 \frac{R_{eq}}{R_L} = \left(\frac{D}{1-D}\right)^2 \frac{R_{eq}}{R_L} \quad (1)$$

Half effect current sensors can be used to provide an alternative path with low power loss and improved accuracy but with high cost and noisy in operation.

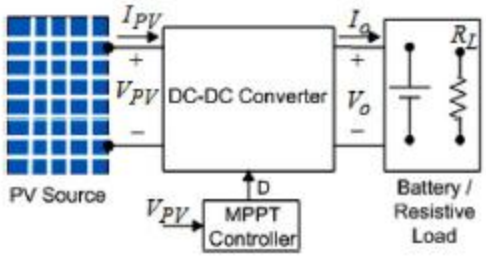

Fig.1. PV system with MPPT

Due to the disadvantage with current sensor, voltage sensor is comparatively better with low power loss and cost. The MPPT with voltage sensor and fixed size is implemented and verified for an interleaved dual boost converter. By considering equation as an objective function an adaptive voltage sensor based MPPT with a constant start up scaling factor has been developed where P is the power of the PV module and D is the duty cycle of the converter. A variable scaling factor is applied in the proposed voltage based adaptive MPPT technique to obtain fast tracking response and reduced steady state oscillation.
The main concern of MPPT technique are steady state behaviour and drift phenomenon used to determine the tracking efficiency. Here proposed adaptive technique, steady state behaviour and drift analysis for the voltage sensor based MPPT method have been implemented.
To increase the range of operation of PV voltage we used single ended primary inductance converter (SPEIC). This has an advantage of non-inverting output polarity, easy to operate and low input current ripple.
V_{PV} is PV voltage and I_{PV} current respectively. The equivalent input resistance R_{eq} of the converter can be calculated using equation 1 as

$$R_{eq} = \eta\left(\frac{1-D}{D}\right)^2 R_L \quad (2)$$

The output power from the PV module which is input power to the converter calculated as

$$P = \frac{V_{PV}^2}{R_{eq}} = \frac{V_{PV}^2}{\eta R_{eq}}\left(\frac{D}{1-D}\right)^2 \quad (3)$$

Fig 2 shows that both P and square root of power (p^*) have the maximum value at the same duty cycle.
Equation used to calculate the maximum power tracking with square root of power (p^*) can be as follows

$$P^* = \sqrt{P} = \frac{V_{PV}}{\sqrt{\eta R_L}}\left(\frac{D}{1-D}\right) \quad (4)$$

At MPP from fig. 2, the slope of the (p^*) curve is zero i.eeqn and it can be calculated as

$$\frac{dP^*}{dD} = \left(V_{PV}\frac{1}{(1-D)^2} + \frac{D}{1-D}\frac{dV_{PV}}{dD}\right)\frac{1}{\sqrt{\eta R_L}} = 0 \quad (5)$$

$$\frac{dP^*}{dD} = \left(-D\frac{V_{PV}dD + D(1-D)dV_{PV}}{(1-D)^2 dD}\right)\frac{1}{\sqrt{\eta R_L}} = 0 \quad (6)$$

Using dP/dD at MPP, the objective function can be determined as

$$Q = D(1-D)dV_{PV} + V_{PV}dD \begin{cases} = 0 & \text{at MPP} \\ > 0, & \text{on left of MPP} \\ < 0, & \text{on right of MPP} \end{cases} \quad (7)$$

Hence, depending on the sign of Q, the MPPT algorithm decides whether to increase or decrease the duty cycle and the corresponding Q-D characteristics are shown in fig.2

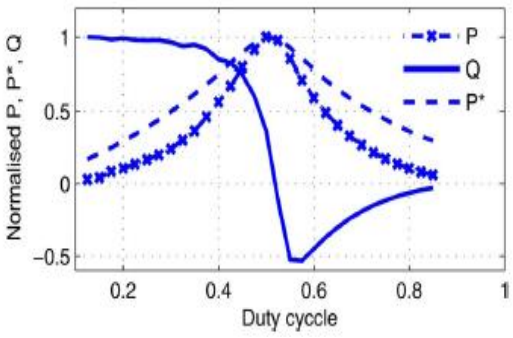

Fig. 2.Normalized variation of *P*, *P*·, *Q*with duty cycle for SEPIC.

B. Case 2: For Battery as a Load

We know P= $V_{PV}I_{PV}$ and hence dP/dD can be calculated as

$$\frac{dP}{dD} = I_{PV}\frac{dV_{PV}}{dD} + V_{PV}\frac{dI_{PV}}{dD} \quad (8)$$

For SPEIC converter, I_{PV} and battery current (I_{bat}) can be calculated as

$$I_{PV} = \frac{D}{1-D} I_{bat} \quad (9)$$

$$\frac{dI_{PV}}{dD} = \frac{1}{(1-D)^2} I_{bat} \quad (10)$$

Putting (9) and (10) in equation (8)

$$\frac{dP}{dD} = \left[\frac{D(1-D)dV_{PV} + V_{PV}dD}{(1-D)^2 dd}\right] I_{bat} \quad (11)$$

By using equation 11 at MPP, the objective function (Q) for tracking the peak power with the battery load can be calculated as same as 7. Thus the voltage sensor based MPPT method is valid for both resistive and battery load.
The objective function Q with boost converter in case of PV system can be obtained by calculating corresponding R_{eq} and dP^*/dD as follows

$$Q = D(1-D)dV_{PV} + V_{PV}dD \begin{cases} = 0, & \text{at MPP} \\ > 0, & \text{on left of MPP} \\ < 0, & \text{on right of MPP} \end{cases} \quad (12)$$

From (7) and (12), it has been observed that the objective function (Q) will vary depending on the dc converter used with PV system. Thus we can conclude that voltage sensor based MPPT is dependent on converter topology where as widely accepted methods such as P&O and IncCond are independent of the converter.

The main factor in any MPPT algorithm is perturbation time and perturbation step size. The selection criterions for these two parameters are as follows:
Choosing proper perturbation (Ta) – Due to step change in duty cycle, the perturbation time should be greater than the setting time of the system. Different values of setting time will result in different values of D. For a maximum step Dmax change in duty cycle which results in perturbation time greater than setting time.
Choosing proper perturbation step size (D) – The perturbation step size should be selected by considering dynamic and steady state performance. The dynamic performance can be improved by using maximum value of step size (Dmax) and smaller value of Dmin results in lower oscillation around the MPP, which improves the steady state performance. The selection criterion for selecting Dmin value is the minimum change in voltage due to perturbation of D by Dmin should be more than the ADC resolution for an N-bit ADC with a maximum value of the ADC channel as VADC. It should satisfy the following condition:

$$\left[V(D+\Delta D_{\min}) - V(D)\right] * S \geq \frac{V_{ADC}}{2^N} \quad (13)$$

Where s is the scaling factor. Here Dmin is chosen as 0.5% for a 10 bit ADC with VADC of 5V that satisfies (13).

C. Adaptive voltage-sensor-based MPPT with variable scaling factor

An adaptive voltage-sensor-based MPPT is used to minimize the solar radiation for maximum power tracking time and power loss in steady state with variable scaling factor. We designate the iterative values of PV voltage and duty cycle of the converter as V_{PV} (K), V_{PV} (K - 1), D (K) and D (K - 1) respectively. The iteration values of voltage and duty cycle are

$$dV_{PV} = V_{PV}(k) - V_{PV}(K-1) \quad (14)$$

$$dD = D(k) - D(k-1) \quad (15)$$

Change of Q decide the operating point and the duty cycle is increased or decreased by ΔD as mentioned in (16). By using sign of Q as +ve then it is incremented and if Q is –ve then duty cycle is decremented by ΔD. Moreover the duty cycle is changed by adjusting the D value. Thus

$$D(k+1) = D(k) \pm \Delta D \quad (16)$$

Q can be plotted in Fig. 3 (a) and (b) with change in insolation from 0 to 270 w/m^2. The fig.3 (a) shows that the value of Q is maximum in start-up and small in steady state. The fixed scaling factor cannot satisfy the requirement of MPPT controller in different conditions so the proposed algorithm uses two different scaling factors M_1 and M_2 to optimally vary the perturbation step size ΔD, which is linear function of Q by

$$\Delta D = M_i Q \quad (17)$$

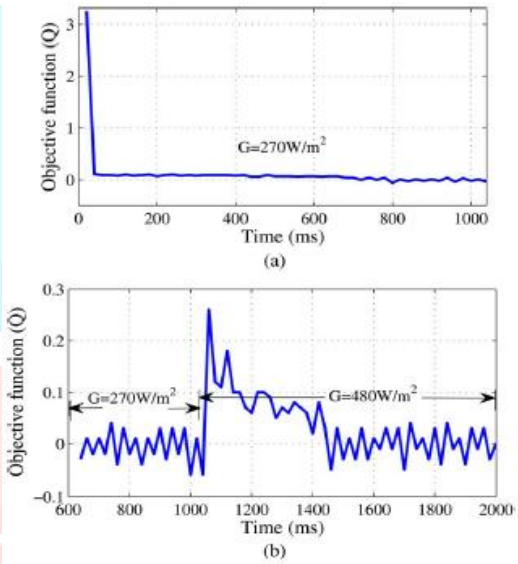

Fig. 3. Variation of Q (a) from start-up to steady state and (b) for a step change in solar insolation.

The scaling factor M_i (I = 1, 2) plays a vital role in an adaptive MPPT method; therefore it should be selected to increase the peak power tracking efficiency. Both M_1 and M_2 are used to reduce the tracking time and power loss in the steady state. Thus the proposed algorithm enhances system performance in terms of transient and steady state.

The scaling factor is selected to generate ΔD depending on the value of Q with respect to a predefined threshold value of the objective function i.e. Q_{th} as factor M_1 and M_2 obey (18) and (19) for maximum and minimum ΔD for proper convergence of the MPPT algorithm. Thus the value of ΔD varies between ΔD_{min} and ΔD_{max} as in equation (20).

$$M_1 Q \leq \Delta D_{max} \quad (18)$$

$$M_2 Q \geq \Delta D_{min} \quad (19)$$

$$\Delta D = \begin{cases} \Delta D_{max}, if\ \Delta D > \Delta D_{max} \\ \Delta D, if\ \Delta D_{max}, \leq \Delta D \leq \Delta D_{min} \\ \Delta D_{min}, if\ \Delta D < \Delta D_{min} \end{cases} \quad (20)$$

Pseudo code for the proposed algorithm:

Initialize V_{PV} (K - 1) and D (K - 1)
Initialize M_1, M_2 and Q_{th}
Loop: Sample and average V_{PV} (K)
Calculate Q

If ($|Q| > Q_{th}$)

$\Delta D = M_1 |Q|$

Or

If ($|Q| < Q_{th}$)

$\Delta D = M_2 |Q|$

If ($Q > 0$)

$D(K+1) = D(K) + \Delta D$

IF ($Q < 0$)

$D(K+1) = D(K) - \Delta D$

Else

No change

Go to loop

D. Steady state analysis

Fig. 4 shows the operating point on Q-D and P-V characteristics. Assume that the operating point during (K - 3) Ta time interval is at point (a). As Q > 0 at point (a), the algorithm increases the duty cycle and hence, the operating point moves to point (b) during (K - 2) Ta time interval. At point (b), the algorithm again increases duty cycle as Q > 0, and the operating point moves to (c). Similarly at point (c), the algorithm increases the duty cycle because Q > 0 and hence the operating point moves to point (d) during KTa time interval. At point (d), as Q < 0, the algorithm decreases the duty cycle and hence the operating point moves back to point (c). Again at point (c), as Q > 0, the algorithm makes the operating point to move to point (d) by increasing duty cycle. Thus in steady state, the operating point moves in two levels resulting power loss minimization compared to P&O and IncCond as in case of P&O and IncCond, the Q moves in three levels as shown in Fig. 5.

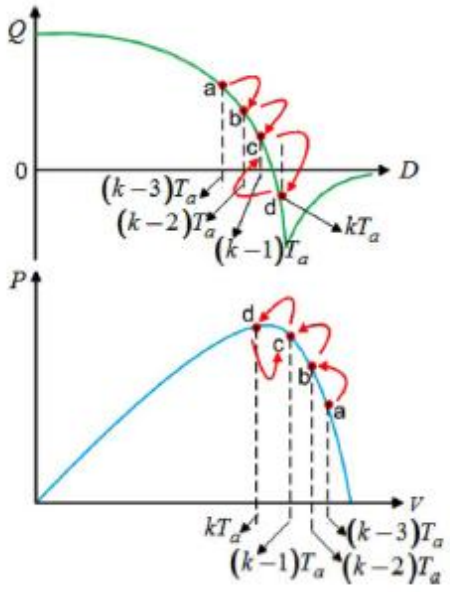

Fig. 4.Movement of the operating point on the Q−DCharacteristics along with P−V characteristics.

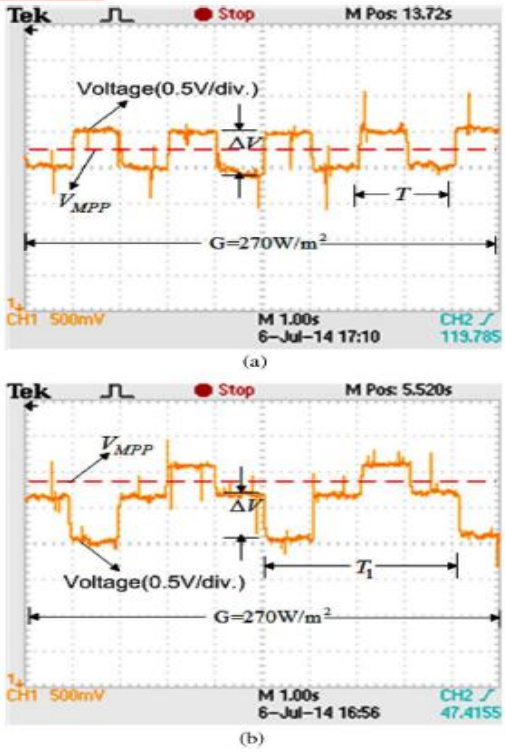

Fig. 5. Steady-state voltage oscillations around the MPP (a) forvoltage-sensor-based MPPT and (b) for P&O MPPT

.

E. Steady state power loss evaluation

The two-level operation of the voltage-sensor-based MPPT algorithm minimizes the voltage oscillations around the MPP, resulting in power loss minimization. The power losses Pr due to oscillation in comparison with the available maximum power (Pmp) are as

$$\frac{P_r}{P_{mp}} = \left(\frac{(\Delta V_{PV})_{RMS}}{V_{MPP}}\right)^2 \left(1 + \frac{V_{MPP}}{2av_t}\right) \tag{21}$$

where (ΔVPV)RMS is the RMS value of steady-state voltage oscillation.
VMPP is the PV module voltage at MPP
A is the diode ideal factor and
Vf is the thermal voltage of the PV module

The voltage oscillation is around the MPP as shown in Fig. 5(a) with the voltage-sensor-based MPPT are given by

$$\Delta V_{PV}(t) = \begin{cases} \frac{1}{2}\Delta V, \text{if } 0 < t < \frac{T}{2} \\ \frac{1}{2}\Delta V, \text{if } \frac{T}{2} < t < T \end{cases} \tag{22}$$

The RMS value of the voltage oscillation is

$$(\Delta V_{PV})_{RMS_{VS}} = \sqrt{\int_0^T (\Delta V_{PV}(t))^2 dt} = \Delta V \frac{1}{2} \tag{23}$$

Putting (23) in (21) gives relative power loss with voltage-sensor based MPPT in steady state as

$$\left(\frac{P_r}{P_{mp}}\right)_{VS} = \frac{1}{4}\left(\frac{\Delta V}{V_{MPP}}\right)^2 \left(1 + \frac{V_{MPP}}{2av_t}\right) \tag{24}$$

From fig 5 (b), the voltage oscillation around the MPP in steady state in case of three-level MPPT algorithm is

$$\Delta V_{PV}(t) = \begin{cases} \frac{3}{2}\Delta V, \text{if } 0 < t \le \frac{T_1}{4} \\ \frac{1}{2}\Delta V, \text{if } \frac{T_1}{4} < t \le \frac{T_1}{2} \\ \frac{1}{2}\Delta V, \text{if } \frac{T}{2} < t < \frac{3T_1}{4} \end{cases} \tag{25}$$

RMS value of the voltage oscillation for P&O is

$$(\Delta V_{PV})_{RMS_{P\&O}} = \sqrt{\int_0^{T_1} (\Delta V_{PV}(t))^2 dt} = \Delta V \frac{\sqrt{3}}{2} \tag{26}$$

Relative power loss with P&O MPPT algorithm can be calculated by using equation (26) and (21) as

$$\left(\frac{P_r}{P_{mp}}\right)_{P\&O} = \frac{3}{4}\left(\frac{\Delta V}{V_{MPP}}\right)^2 \left(1 + \frac{V_{MPP}}{2av_t}\right) \tag{27}$$

The PV module considered with specification VMPP = 15.5 V at 270 w/m2 insolation, the voltage oscillations around the MPP are ΔV = 0.5 V as shown in Fig. 5. Relative power loss can be obtained by using eqn (24) and (27) respectively.

$$\left(\frac{P_r}{P_{mp}}\right)_{VS} = 0.19 \tag{28}$$

$$\left(\frac{P_r}{P_{mp}}\right)_{P\&O} = 0.57 \tag{29}$$

$$\eta_{MPPT} = \left(1 - \left(\frac{P_r}{P_{MPP}}\right)\right) \times 100\,\% \tag{30}$$

Tracking efficiency of voltage-sensor-based MPPT i.e. by considering only the power loss due to voltage oscillation around MPP in steady state can be calculated by using (28) and (29) in (30) as

$$\eta_{VS} = 99.81\ \% \tag{31}$$

$$\eta_{p\&o} = 99.43\ \% \tag{32}$$

Thus the relative power loss for voltage-sensor-based MPPT is only 0.19% of maximum power which is available and is 1/3rd of the power loss for other MPPT methods with three level steady state operations. With this method we achieve good energy efficiency from past 25 years.

F. Drift Analysis

Drift means movement of the operating point in opposite direction for a change in insolation and the drift problem occurs in case of change in radiation with P&O and IncCond methods, it is discussed in [18]-[20], [22]. However drift analysis for voltage-sensor-based MPPT is not discussed in literature.
The drift analysis can be examined by calculating the change in operating point voltage VPV and the objective function Q for a change in insolation.

Relationship between IPV and VPV corresponding to the present operating point on the I-V characteristics of the PV module with SEPIC converter can be expressed in terms of slope of the load line as

$$I_{PV} = \frac{D^2}{\eta R_L (1-D)^2} V_{PV} \tag{33}$$

From the ideal single-diode of the PV model, IPV and VPV can be expressed as

$$I_{PV} = I_{SC} - I_{rs}\left(e^{\frac{V_{PV}}{av_t}} - 1\right) \tag{34}$$

Where,
ISC is the short circuit current
IRS is the reverse saturation current

Now VPV can be expressed in terms of ISC for an insolation G1 as follows

$$V_{PV_{G_1}} = \frac{I_{SC\,G_1}}{\frac{D^2}{\eta R_L (1-D)^2} + \frac{I_{rs}}{av_t}} \tag{35}$$

Consider change in insolation from G1 to G2 in between perturbation time while operating with a certain duty cycle. Then change in operating point voltage can be calculated as –

$$V_{PV_{G2}} = \frac{I_{SC\,G_2}}{\frac{D^2}{\eta R_L (1-D)^2} + \frac{I_{rs}}{av_t}} \tag{36}$$

From (35) and (36), it can be noticed that, for an increase in insolation, VPV increases as Isc increases, and the change in VPV due to insolation change can be obtained as follows:

$$\Delta V_{PV_G} = \frac{I_{SC_{G_2}} - I_{SC_{G_1}}}{\frac{D^2}{\eta R_L (1-D)^2} + \frac{I_{rs}}{av_t}} \tag{37}$$

By using (36) and (37) in (7), the objective function Q due to change in insolation with certain duty cycle can be expressed as

$$Q = D(1-D)\frac{I_{SC_{G_2}} - I_{SC_{G_1}}}{\frac{D^2}{\eta R_L (1-D)^2} + \frac{I_{rs}}{av_t}} + \frac{I_{SC\,2_{G_2}}}{\frac{D^2}{\eta R_L (1-D)^2} + \frac{I_{rs}}{av_t}}\,\mathrm{Dd} \tag{38}$$

From (38) it can be concluded that Q is +ve for an increase in insolation and Q is –ve for a decrease in insolation as Isc is directly proportional to the insolation level. Here MPPT algorithm will take decision based on the sign of Q. For an increase in insolation the algorithm increases the duty cycle i.e. moving to the MPP and vice versa. Thus the voltage-sensor-based MPPT method is free from drift for both increase and decrease in insolation condition.

Fig. 6. Shows drift analysis. As increase in insolation while operating point is at (d), then the operating point will be settled to a new point (e) on the Q-D or the P-V characteristics corresponding to the increased insolation.

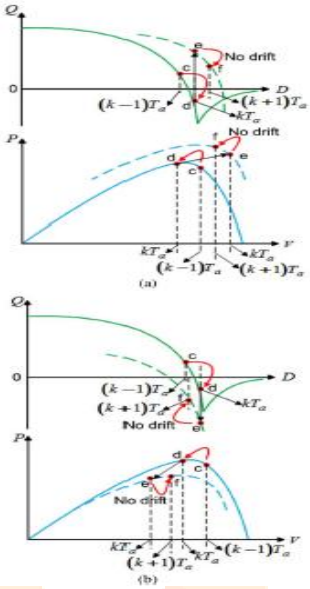

Fig. 6. Drift analysis with Q−D and P−V characteristics (a) for a step increase in insolation and (b) for a step decrease in insolation.

Using algorithm take decision to increase the duty cycle as Q > 0 at point (e) and thereby the operating point moves closer to the MPP at point (f). Thus the voltage-sensor-based MPPT method is free from drift in case of increase in insolation. Similarly, for a decrease in insolation the operating point at (d). Shown in fig 6 (b) the operating point will be settled to a new point (e) on the Q-D or P-V curve corresponding to the decreased insolation. As I < 0 at point (e), the algorithm decreases the duty cycle and hence the operating point moves closer to the MPP (point (f)). Thus the voltage-sensor-based MPPT algorithm is free from drift for both increase and decrease in insolation.

III. SIMULATION RESULT

The proposed MPPT algorithm has been tested for a step change in insolation level from 270 to 480 W/m2 at 0.1 s. The perturbation time and the perturbation step size for the fixed-step-size method are chosen as 20 ms and 0.5%, respectively. The P−V characteristics of the simulated PV module are shown in Fig. 7. From the simulated P−V characteristics, it can be noticed that the MPP voltages are 15.13 and 16.16 V, corresponding to the insolation level of 270 and 480 W/m2, respectively. The tracking waveforms with the fixed-step-size method and with the proposed adaptive method are shown in Fig. 8, and it can be visualized that both methods are efficiently tracking the corresponding MPP voltage, but the tracking time is larger in the case of the fixed-step-size method. Fig. 8(a) shows that the tracking time with the fixed-step-size method in start-up case for G = 270 W/m2 is T1 = 600 ms, and it has been reduced to 130 ms with the proposed adaptive method.

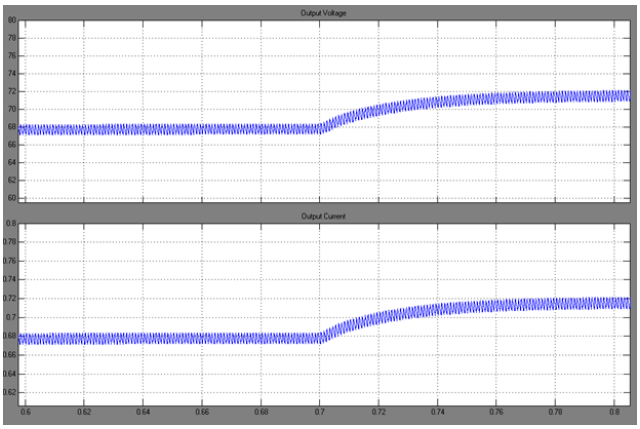

Fig.7. Adaptive Method (Adaptive Step size) at 0.7sec, irradiance from 270w/m2 to 480w/m2

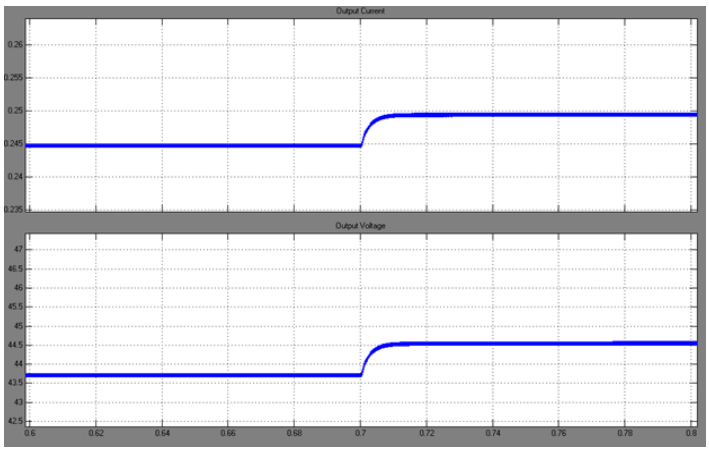

Fig. 8. P & O Method (Fixed Step size) at 0.7sec, irradiance from 270w/m2 to 480w/m2

CONCLUSION

In this paper, an adaptive voltage-sensor-based MPPT algorithm with variable scaling factor by considering direct duty cycle control method for SEPIC converter has been implemented. The proposed system is designed, and the functionality of MPPT control has been proved. The simulation results prove that the proposed system is able to track the maximum power from the PV module; moreover, the steady-state two-level operation and the drift-free phenomena are the merits of this tracking algorithm. Hence, this method improves the efficiency of the PV system and reduces power loss in steady state. From the results obtained, it is noticed that, with a well-designed system, including a proper converter and an efficient MPPT algorithm, the MPPT can be developed with less complexity and reduced cost.

REFERENCES

[1] M. G. Villalva, J. R. Gazoli, and E. R. Filho, "Comprehensive approachto modeling and simulation of photovoltaic arrays," IEEE Trans. Power Electron., vol. 24, no. 5, pp. 1198–1208, May 2009.

[2] J. H. R. Enslin, M. S. Wolf, D. B. Snyman, and W. Swiegers, "Integrated photovoltaic maximum power point tracking converter," IEEE Trans. Ind. Electron., vol. 44, no. 6, pp. 769–773, Dec. 1997.

[3] M. A. S. Masoum, H. Dehbonei, and E. F. Fuchs, "Theoretical and experimental analyses of photovoltaic systems with voltage and current-based maximum power-point tracking," IEEE Trans. Energy Convers., vol. 17, no. 4, pp. 514–522, Dec. 2002.

[4] W. Xiao and W. G. Dunford, "A modified adaptive hill climbing MPPT method for photovoltaic power systems," in Proc. IEEE PESC, 2004, pp. 1957–1963.

[5] D. Sera, R. Teodorescu, J. Hantschel, and M. Knoll, "Optimized maximum power point tracker for fast-changing environmental conditions," IEEE Trans. Ind. Electron., vol. 55, no. 7, pp. 2629–2637, Jul. 2008.

[6] K. L. Lian, J. H. Jhang, and I. S. Tian, "A maximum power point tracking method based on perturb-and-observe combined with particle swarm optimization," IEEE J. Photovoltaics, vol. 4, no. 2, pp. 626–633, Mar. 2014.

[7] F. Liu, S. Duan, B. Liu, and Y. Kang, "A variable step size INC MPPT method for PV systems," IEEE Trans. Ind. Electron., vol. 55, no. 7, pp. 2622–2628, Jul. 2008.

[8] A. Safari and S. Mekhilef, "Simulation and hardware implementation of incremental conductance MPPT with direct control method using Cuk converter," IEEE Trans. Ind. Electron., vol. 58, no. 4, pp. 1154–1161, Apr. 2011.

[9] K. S. Tey and S. Mekhilef, "Modified incremental conductance algorithm for photovoltaic system under partial shading conditions and load variation," IEEE Trans. Ind. Electron., vol. 61, no. 10, pp. 5384–5392, Oct. 2014.

[10] Q. Mei, M. Shan, L. Liu, and J. M. Guerrero, "A novel improved variable step-size incremental-resistance MPPT method for PV systems," IEEE Trans. Ind. Electron., vol. 58, no. 6, pp. 2427–2434, Jun. 2011.

[11] T. Esram, J. W. Kimball, P. T. Krein, P. L. Chapman, and P. Midya, "Dynamic maximum power point tracking of photovoltaic arrays using ripple correlation control," IEEE Trans. Power Electron., vol. 21, no. 5, pp. 1282–1291, Sep. 2006.

[12] T. Wu, C. Chang, and Y. Chen, "A fuzzy-logic-controlled single-stage converter for PV-powered lighting system applications," IEEE Trans. Ind. Electron., vol. 47, no. 2, pp. 287–296, Apr. 2000.

[13] Syafaruddin, E. Karatepe, and T. Hiyama, "Artificial neural network-polar coordinated fuzzy controller based maximum power point tracking control under partially shaded conditions," IET Renew. Power Gener., vol. 3, no. 2, pp. 239–253, Jul. 2009.

[14] K. Ishaque and Z. Salam, "A deterministic particle swarm optimization maximum power point tracker for photovoltaic system under partial shading condition," IEEE Trans. Ind. Electron., vol. 60, no. 8, pp. 3195–3206, Aug. 2013.

[15] E. Bianconi et al., "A fast current-based MPPT technique employing sliding mode control," IEEE Trans. Ind. Electron., vol. 60, no. 3, pp. 1168–1178, Mar. 2013.

[16] E. Mamarelis, G. Petrone, and G. Spagnuolo, "Design of a sliding mode controlled SEPIC for PVMPPT applications," IEEE Trans. Ind. Electron., vol. 61, no. 7, pp. 3387–3398, Jul. 2014.
[17] T. Esram and P. L. Chapman, "Comparison of photovoltaic array maximum power point tracking techniques," IEEE Trans. Energy Convers., vol. 22, no. 2, pp. 439–449, Jun. 2007.
[18] D. P. Hohm and M. E. Ropp, "Comparative study of maximum power point tracking algorithms," Prog. Photovoltaics Res. Appl., vol. 11, no. 1, pp. 47–62, Apr. 2003.
[19] N. Femia, G. Petrone, G. Spagnuolo, and M. Vitelli, "Optimization of perturb and observe maximum power point tracking method," IEEE Trans. Power Electron., vol. 20, no. 4, pp. 963–973, Jul. 2005.
[20] M. A. Algendy, B. Zahawi, and D. J. Atkinson, "Assessment of perturb and observe MPPT algorithm implementation techniques for PV pumping applications," IEEE Trans. Sustain. Energy, vol. 3, no. 1, pp. 21–33, Jan. 2012.
[21] K. H. Hussein, I. Muta, T. Hoshino, and M. Osakada, "Maximum photovoltaic power tracking: An algorithm for rapidly changing atmospheric conditions," Proc. Inst. Elect. Eng.—Gener.,Transmiss. Distrib., vol. 142, no. 1, pp. 59–64, Jan. 1995.
[22] D. Sera, L. Mathe, T. Kerekes, S. V. Spataru, and R. Teodorescu, "On the perturb-and-observe and incremental conductance MPPT methods for PV systems," IEEE J. Photovoltaics, vol. 3, no. 3, pp. 1070–1078,Jul. 2013.